

10/12-10-96 JS(1)

LBNL-39307
UC-414



ERNEST ORLANDO LAWRENCE BERKELEY NATIONAL LABORATORY

Noise Analysis due to Strip Resistance in the ATLAS SCT Silicon Strip Module

I. Kipnis
Engineering Division

August 1996



DISCLAIMER

Portions of this document may be illegible in electronic image products. Images are produced from the best available original document.

DISCLAIMER

This document was prepared as an account of work sponsored by the United States Government. While this document is believed to contain correct information, neither the United States Government nor any agency thereof, nor The Regents of the University of California, nor any of their employees, makes any warranty, express or implied, or assumes any legal responsibility for the accuracy, completeness, or usefulness of any information, apparatus, product, or process disclosed, or represents that its use would not infringe privately owned rights. Reference herein to any specific commercial product, process, or service by its trade name, trademark, manufacturer, or otherwise, does not necessarily constitute or imply its endorsement, recommendation, or favoring by the United States Government or any agency thereof, or The Regents of the University of California. The views and opinions of authors expressed herein do not necessarily state or reflect those of the United States Government or any agency thereof, or The Regents of the University of California.

Available to DOE and DOE Contractors
from the Office of Scientific and Technical Information
P.O. Box 62, Oak Ridge, TN 37831
Prices available from (615) 576-8401

Available to the public from the
National Technical Information Service
U.S. Department of Commerce
5285 Port Royal Road, Springfield, VA 22161

Ernest Orlando Lawrence Berkeley National Laboratory
is an equal opportunity employer.

LBNL-39307
UC-414

Noise Analysis due to Strip Resistance in the ATLAS SCT Silicon Strip Module

Issy Kipnis
Lawrence Berkeley National Laboratory
University of California
Berkeley, CA 94720

This work was supported by the Director, Office of Energy Research,
Office of High Energy and Nuclear Physics, Division of High Energy
Physics of the U.S. Dept. of Energy under contract No. DE-AC03-
76SF00098

DISTRIBUTION OF THIS DOCUMENT IS UNLIMITED

129
MASTER

Noise Analysis due to Strip Resistance in the ATLAS SCT Silicon Strip Module

Issy Kipnis
Lawrence Berkeley National Laboratory

Introduction

This note presents the noise analysis due to strip resistance in the ATLAS SCT silicon strip module. The module is made out of four 6 cm x 6 cm single sided silicon microstrip detectors. Two detectors are butt glued to form a 12 cm long mechanical unit and strips of the two detectors are electrically connected to form 12 cm long strips. The butt gluing is followed by a back to back attachment. The module under consideration in this note is the Rφ module where the electronics is oriented parallel to the strip direction and bonded directly to the strips. It has been stated before that this module concept provides the maximum signal-to-noise ratio, in particular, when placing the front-end electronics near the middle of the module unit (as opposed to placing the electronics at the end of the strips) to reduce the effective series strip resistance and to minimize signal dispersion through the strips.

The noise originating in the distributed strip resistance contributes to the total noise. To understand its effect on noise, two types of analyses will be performed and compared. First, the equivalent series impedance Z_{eq} in a uniformly distributed RC line and in the full detector model will be determined analytically and numerically. Second, the noise contribution of the distributed strip resistance will be determined by a SPICE simulation with a full detector model and multiple channels of the CAFE-bn [1] circuit, comparing the noise performance of end- and center-tapped detector modules for a range of strip resistances.

Uniformly distributed RC line

A useful and convenient approach in analyzing the electrical properties of a long strip detectors is to view them as distributed RC lines where an elementary section of such a line can be represented by an equivalent circuit with a series R representing the metal strip resistance per unit length, and a shunt C representing the capacitance per unit length (Figure 1).

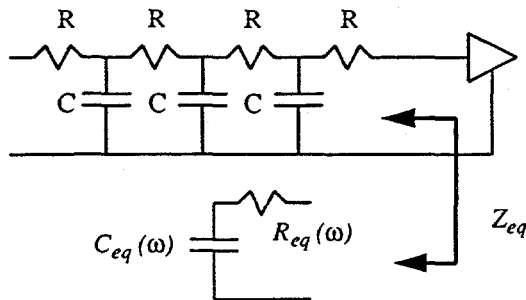


Figure1. Distributed RC line equivalent circuit.

For the analysis of the amplifier noise we are interested in finding out what is the equivalent impedance that the amplifier “sees” looking into the detector, i.e., what is the input impedance of the uniform distributed RC line when its output port is open-circuited, which is given by [2]

$$Z_{eq} = z_{11} = \frac{1}{\sqrt{s}} \sqrt{\frac{R}{C}} \coth(a\sqrt{s}) \quad (1)$$

with

$$a = l\sqrt{RC} = \sqrt{R_t C_t} \quad (2)$$

where l is the total line length, $R_t = lR$ is the total resistance and $C_t = lC$ is the total capacitance.

For $s = j\omega$ the equivalent series resistance and capacitance can be written as

$$R_{eq} = R_t \frac{1}{x} \frac{\sinh x - \sin x}{\cosh x - \cos x} \quad C_{eq} = C_t \frac{2}{x} \frac{\cosh x - \cos x}{\sinh x + \sin x} \quad (3)$$

with

$$x = \sqrt{2\omega R_t C_t} \quad (4)$$

Figure 2 shows the simulation result for the equivalent resistance and capacitance of a distributed RC line with the parameters of the 12 cm strip detector. An interesting observation from the figure is that although the capacitance decreases at high frequencies and the resistance increases at low frequencies, the impedance is flat over a relatively wide frequency range (about 2 decades) corresponding to approximately $0.1 < x < 1$. Performing a Taylor expansion on the trigonometric and hyperbolic functions of (3) in this frequency range, reduces the terms to

$$R_{eq} \approx \frac{R_t}{3} \quad C_{eq} \approx C_t \quad \text{for } 0.1 < x < 1 \quad (5)$$

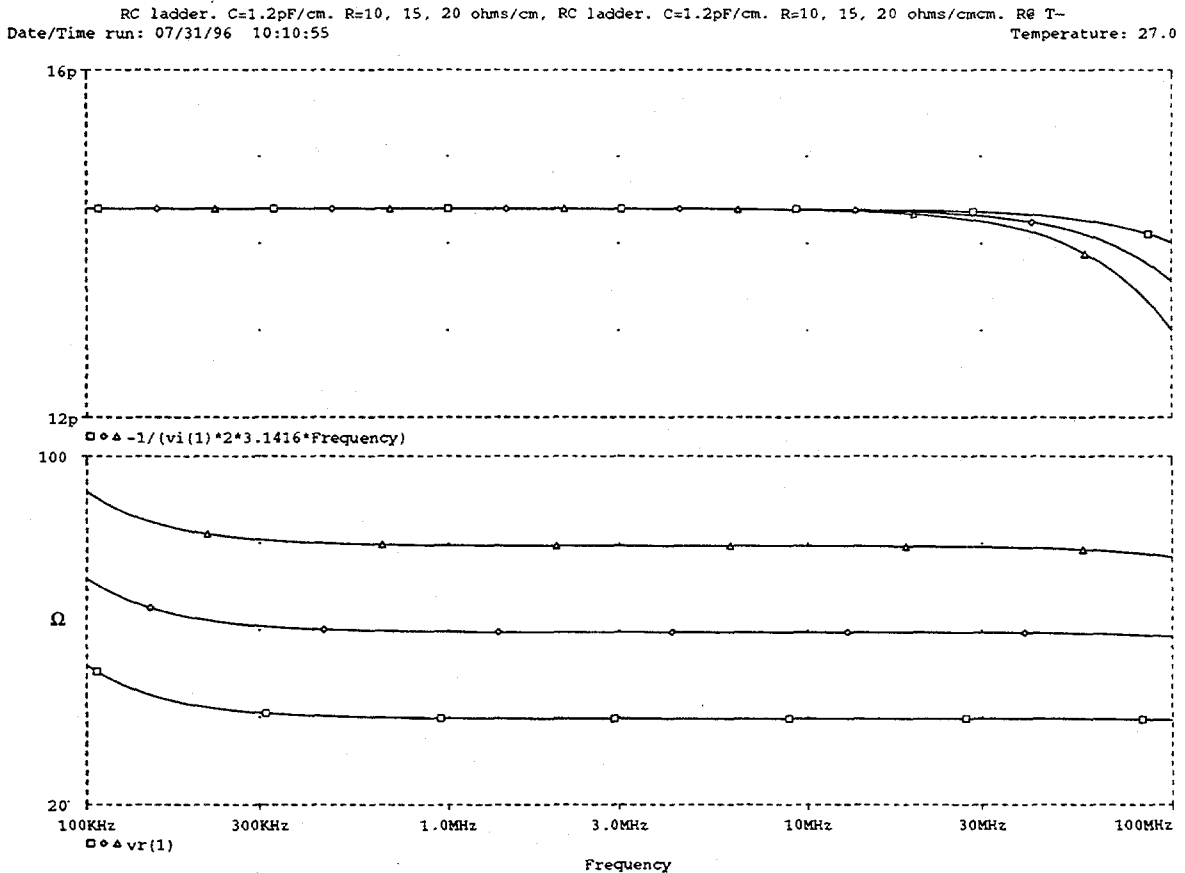


Figure 2. Equivalent capacitance and resistance for an end-tapped 12 cm long distributed RC line with $C = 1.2$ pF/cm and $R = 10, 15$ and 20 Ω /cm.

There is very good agreement between equation (5) and Figure 2. Since we are interested in investigating the performance of the module when the front-end chips are center-tapped to the detector, we would like to know the equivalent series resistance and capacitance when looking at the mid-point, i.e., at the junction of the two detectors. The load impedance of this configuration results from two lines of 6 cm length connected in parallel. The results are

shown in Figure 3. Although the capacitance remains the same, the equivalent series resistance is decreased by approximately a factor of 4, that is

$$R_{eq}|_{end-tap} \approx 4R_{eq}|_{center-tap} \quad (6)$$

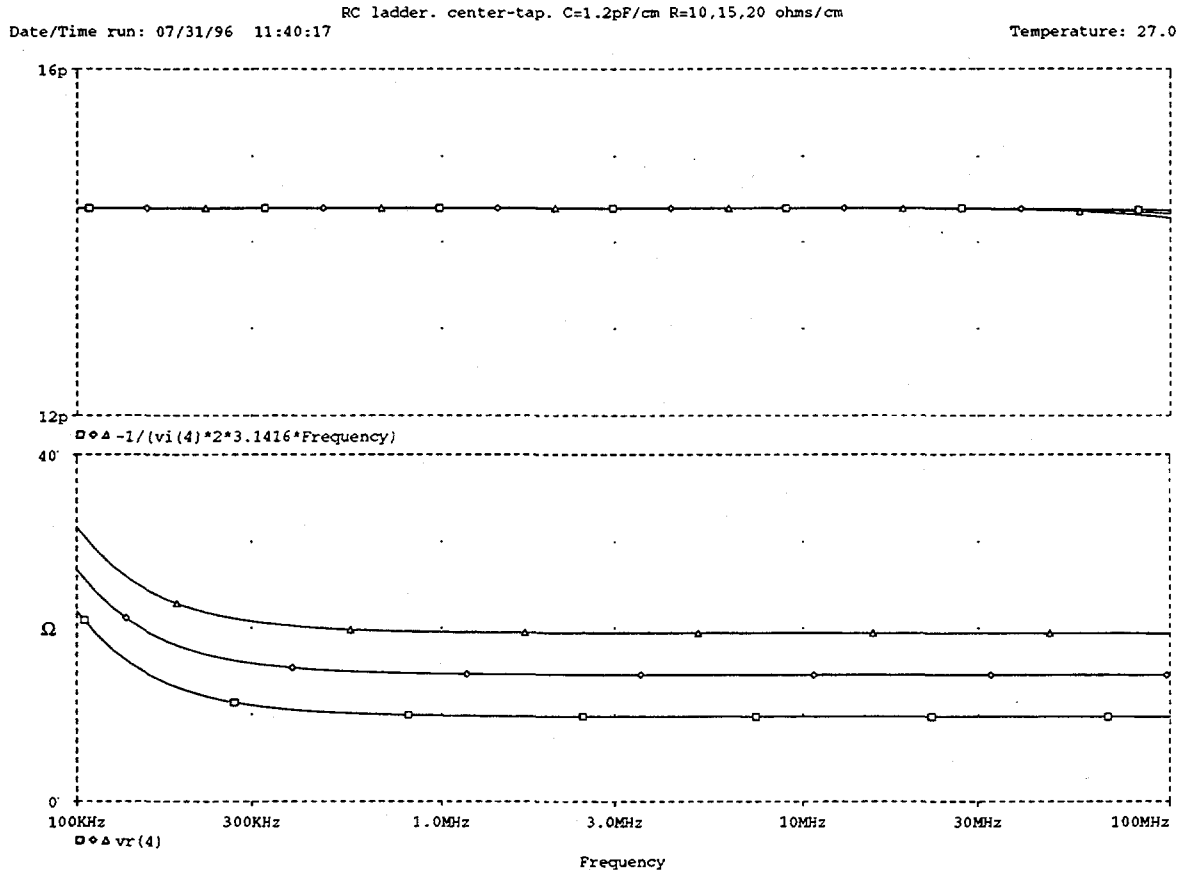


Figure 3. Equivalent capacitance and resistance for a center-tapped 12 cm long distributed RC line with $C = 1.2$ pF/cm and $R = 10, 15$ and 20 Ω /cm.

The equivalent series resistance R_{eq} calculated here is not necessarily equal to the equivalent noise resistance R_n whose contribution to the total noise will be determined from a full SPICE simulation. To get a feeling for the magnitude of the problem regarding noise performance, the equivalent series resistance of the detector contributes to the total noise exactly in the same proportion as the base resistance of the input bipolar transistor (Q_1) in the charge-sensitive preamplifier (see [1], Figure 6). The size of Q_1 is determined by the desired base resistance on one hand, favoring a large transistor, and by β degradation with irradiation on the other hand, which favors a small device. In the CAFE-bn, Q_1 has a base resistance of 20Ω . Clearly, if the detector equivalent noise resistance is much higher than this value, its effect on total noise will be considerable.

Full detector model

We now move from the simple distributed RC line to a full detector model. Figure 4 shows the unit element used in this distributed model. The complete model is built by cascading the proper number of units. Table 1 contains the detector element values used for the simulations for the initial condition and after an irradiation of 10^{14} p/cm². Although not shown in the unit element model, the effects of leakage current and bias resistance are also included in the model.

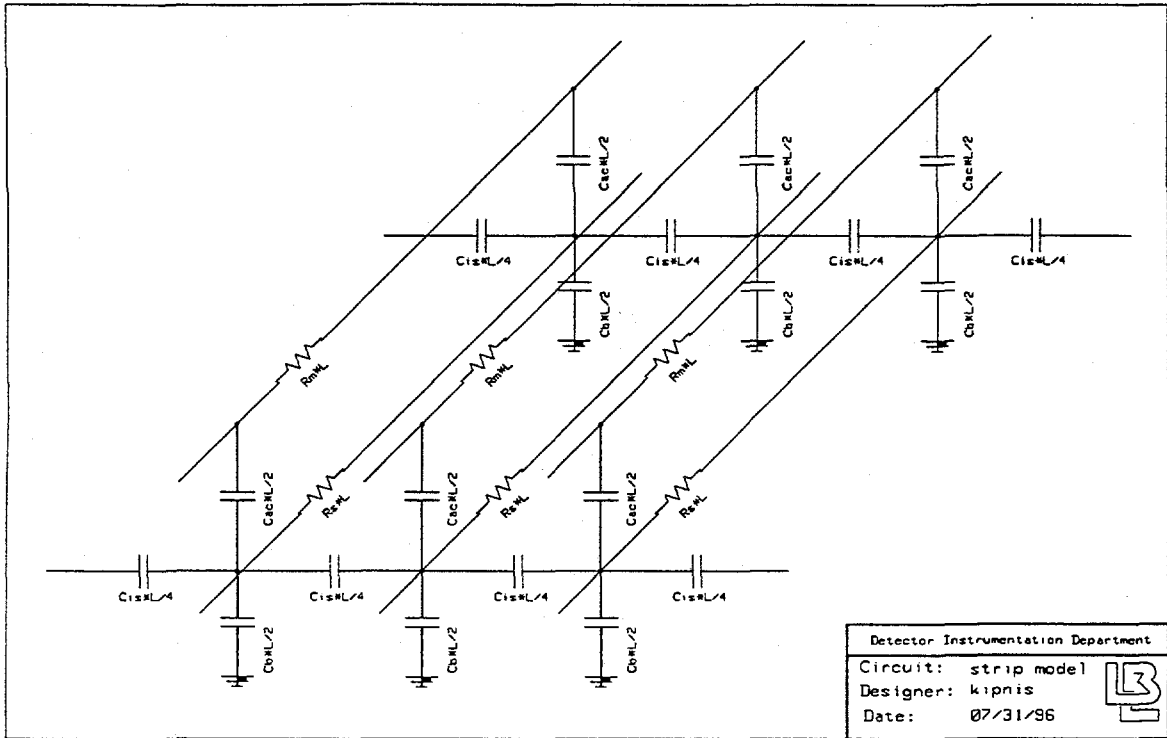
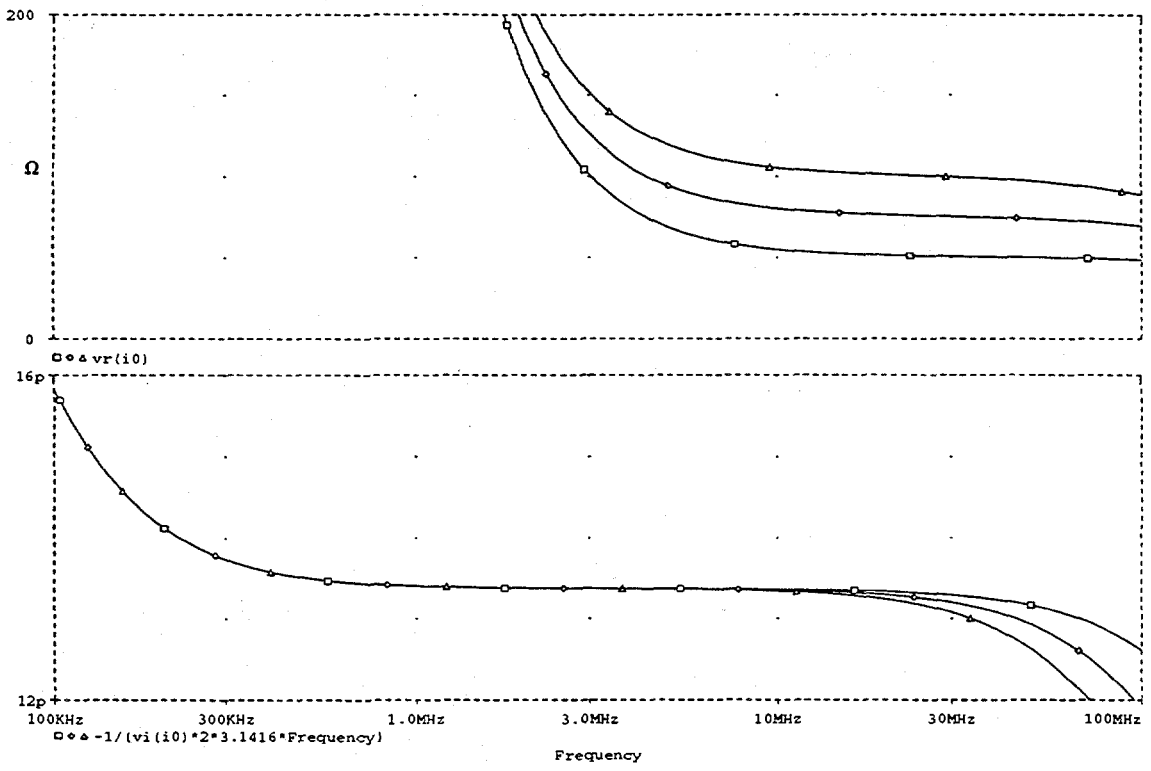


Figure 4. Unit element of the detector distributed model.

Total strip capacitance (pre-irradiation)		1.5	pF/cm
to backplane	C_b	0.28	pF/cm
to both neighbor strips	C_{is}	1.22	pF/cm
Total strip capacitance (post-irradiation)		1.2	pF/cm
to backplane	C_b	0.28	pF/cm
to both neighbor strips	C_{is}	0.92	pF/cm
Coupling capacitance	C_{ac}	20	pF/cm
Metal strip resistance	R_m	20	Ω/cm
Implant strip resistance	R_s	100	$k\Omega/cm$
Bias resistance / 6 cm detector unit	R_b	1.5	$M\Omega$
Leakage current / 12 cm strip (pre-irradiation)	I_l	2	nA
Leakage current / 12 cm strip (post-irradiation)	I_l	2	μA

Table 1: Detector parameters, pre-irradiation and after irradiation to 10^{14} p/cm².

Date/Time run: 07/31/96 14:55:23 end-tapped 12 cm detector. $R_m=10, 15, 20$ ohms/cm Temperature: 27.0



Date/Time run: 07/31/96 14:51:54 center-tapped 12 cm detector. $R_m=10, 15, 20$ ohms/cm Temperature: 27.0

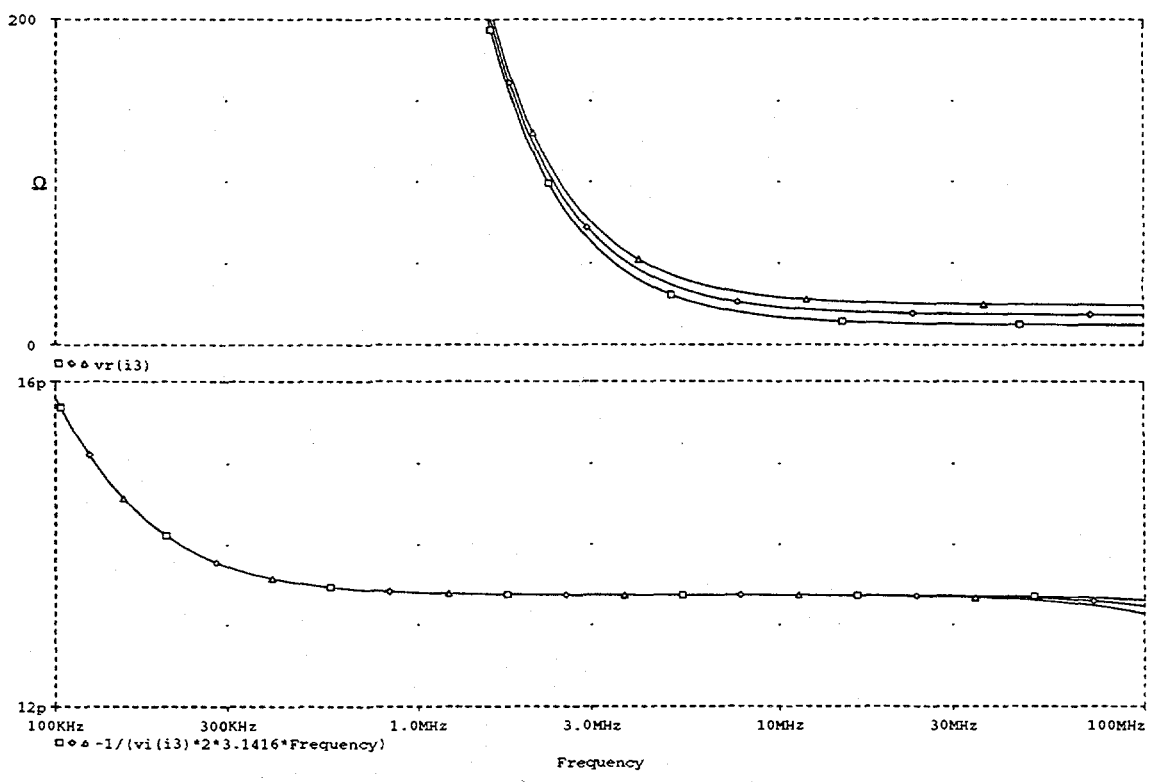


Figure 5. Equivalent resistance and capacitance for a post-irradiated end- and center-tapped full detector models with $R_m = 10, 15$ and $20 \Omega/cm$.

Figure 5 shows the equivalent resistance and capacitance for the post-irradiation center- and end-tapped detectors using the full model. For both cases the equivalent capacitance is about 13.5 pF, which is the series combination of the total strip capacitance (14.4 pF) and the total blocking capacitance (240 pF). The behavior is not as flat as with the simple RC line, but at the frequency range of interest, around 15 MHz (see below), all curves are in their flat regions. Table 2 summarizes the results of the equivalent resistance for the post-rad full detector model. Although the equivalent resistance is somewhat higher than estimated with the simple transmission line model (equation 5), it is directly proportional to R_t , and the ratio of end-tapped to center-tapped resistance is still about 4.

Metal Strip Resistance [Ω/cm]	Equivalent Series Resistance, R_{eq} [Ω]	
	center-tap	end-tap
10	15	53
15	21	78
20	27	103

Table 2: Equivalent series resistance at 15 MHz for the post-irradiated full detector model.

The frequency range of interest is around 15 MHz, where the small-signal transfer gain, from the input of the preamplifier to the input of the comparator, of the CAFE-bn peaks (Figure 6a). Considering the multiple integrations of the response, the time-domain pulse response exhibits a 20 ns peaking time, as shown in the voltage waveform at the input of the comparator in Figure 6b.

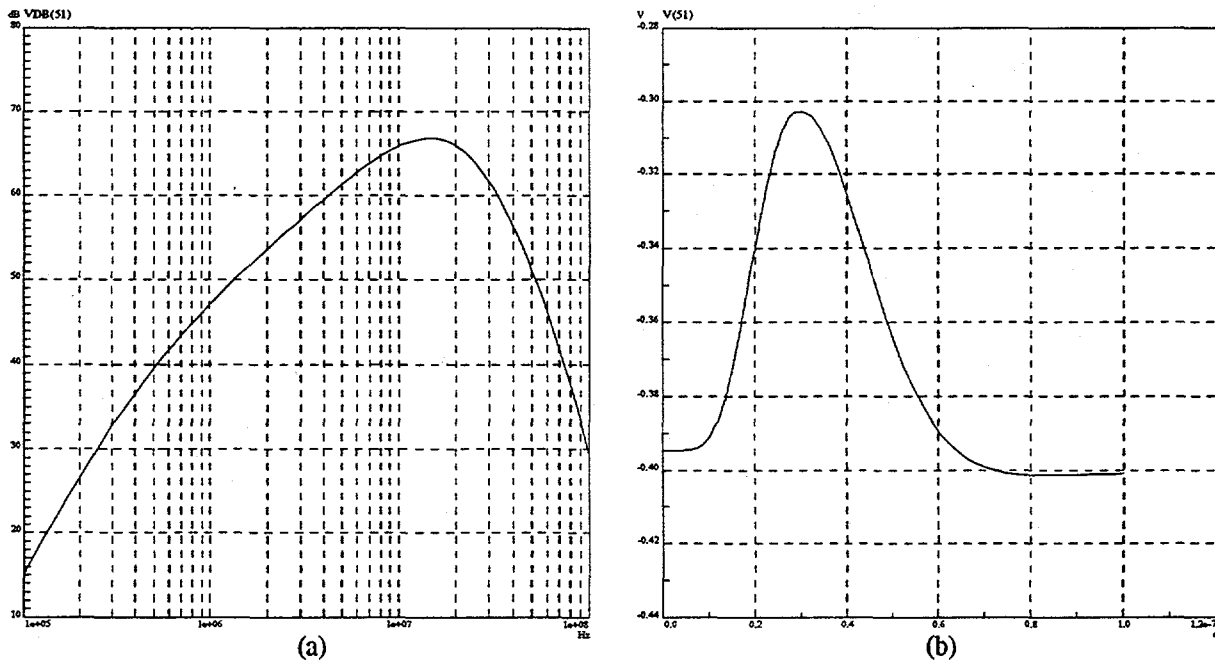


Figure 6. CAFE-bn (a) small signal frequency response and (b) time-domain pulse response to a 1 fC input charge.

Noise Analysis

We now proceed to the noise analysis of the module consisting of the full detector model with pre- and post-irradiation parameters as specified in Table 1 and the CAFE-bn as the front-end electronics. In the simulations, the only

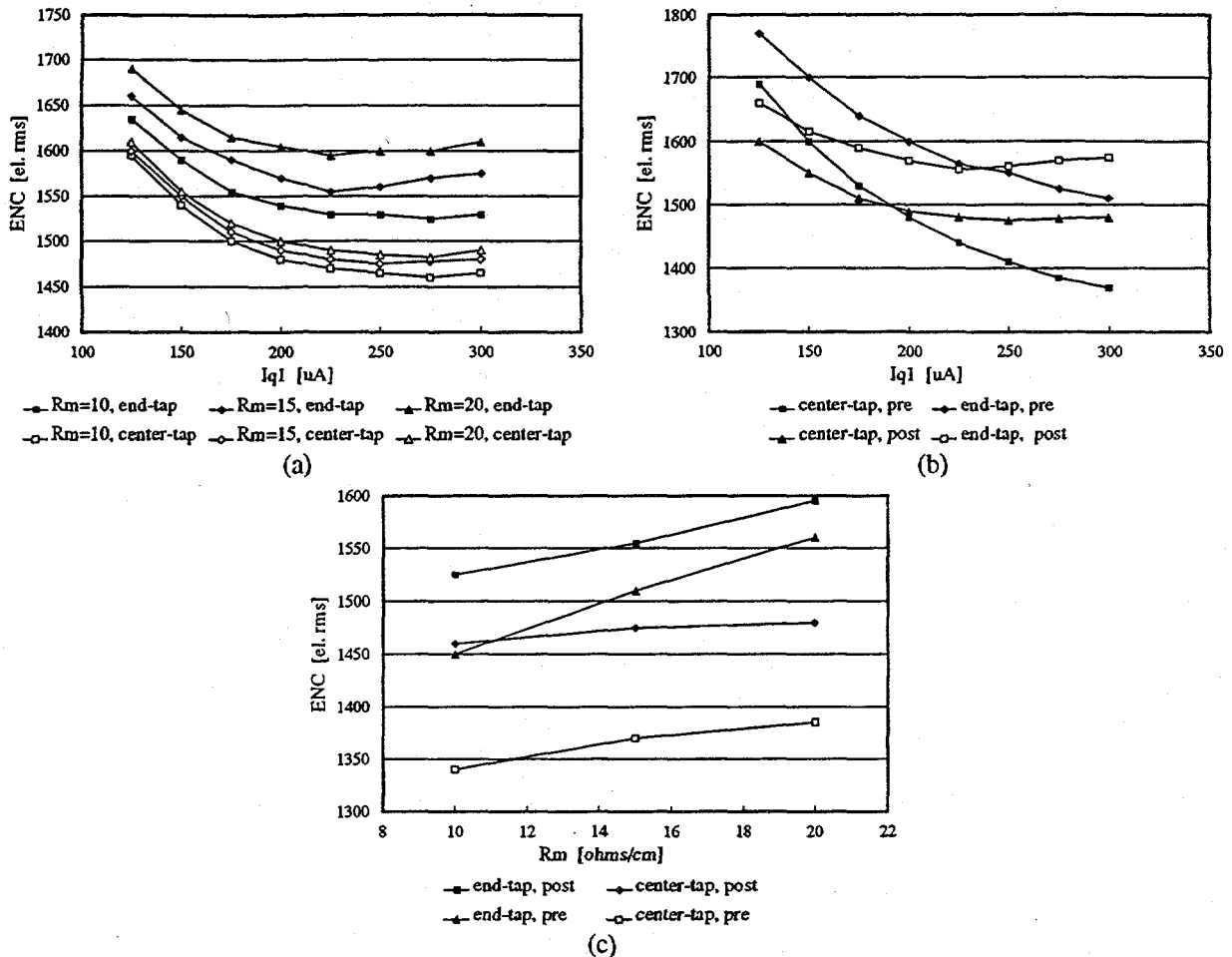


Figure 7. (a) ENC vs. I_{q1} with R_m as a parameter for post-irradiation case. (b) ENC vs. I_{q1} for $R_m = 15 \Omega/cm$. (c) minimum ENC vs. R_m .

parameter in the CAFE circuit that was modified with respect to irradiation was the current gain (β) of the transistors as specified in Table 3. Points of particular importance in the noise analysis are:

- all simulations were performed with 3 channels of electronics to include the noise contributions of neighbor channels
- a simulated n-strip detector current waveform was used as the stimulus to the circuit, rather than a delta impulse, i.e., the simulation includes ballistic deficit

	pre-irradiation	post-irradiation
β_{npn}	120	50
β_{pnp}	40	25

Table 3: CAFE transistor parameters modified for irradiation.

Figure 7a shows the equivalent noise charge (ENC) in electrons rms versus collector I_{q1} current of the input transistor (labeled I_{V11} in [1]) with the metal strip resistance as a parameter for the post-irradiation case. Figure 7b shows the ENC versus I_{q1} for $R_m = 15 \Omega/cm$. Figure 7c shows minimum ENC versus R_m . The minimum value of ENC for the post-irradiation case is achieved at collector currents $I_{q1} \sim 250 \mu A$. For the pre-irradiation case, the ENC shown in

Figure 7c is for $I_{q1} = 300 \mu\text{A}$, although a somewhat lower value for ENC can be achieved at higher currents, as can be seen from the slope of the curves in Figure 7b. Table 4 summarizes the results of the noise analysis.

R_m	post-irradiation			pre-irradiation			Ω/cm
	10	15	20	10	15	20	
ENC, center-tap	1,460	1,475	1,480	1,340	1,370	1,385	el. rms
ENC, end-tap	1,525	1,555	1,595	1,450	1,510	1,560	el. rms
Δ ENC	65	80	115	110	140	175	el. rms
$\% \Delta$ ENC	4.4	5.4	7.8	8.2	10.2	12.6	%

Table 4: Minimum ENC summary.

It is enlightening to see how the different elements in the detector and in the front-end IC contribute to the total noise. Table 5 contains the relative contributions of these elements to the total noise power (in V^2). The elements in the table account for approximately 95% of the total noise in all cases.

	center-tap pre-irradiation	end-tap pre-irradiation	center-tap post-irradiation	end-tap post-irradiation
Transistor Q_1 , main channel	61.8	48.7	60.5	53.1
Transistor Q_1 , neighbor channels	13.5	9.8	6.7	5.4
Metal resistance, main strip	7.0	21.8	3.7	12.7
Metal resistance, neighbor strips	2.3	7.1	1.1	3.8
Feedback resistor R_1 , main channel	6.2	5.3	6.2	5.6
Leakage current, main strip	-	-	12.2	11.0
Resistor R_2 , main channel	2.5	1.9	1.7	1.4
Transistor Q_4 , main channel	1.1	1.0	1.2	1.1
Transistor Q_2 , main channel	-	-	1.5	1.3

Table 5: Percent contribution to total noise power, $I_{q1} = 250 \mu\text{A}$, $R_m = 15 \Omega/\text{cm}$.
Transistor designations as in the CAFE circuit diagram [1].

Also from this analysis the value of the equivalent noise resistance R_n due to the distributed strip resistance can be obtained (Table 6). Although the equivalent noise resistance is lower than the equivalent series resistance of the full detector model (Table 2), it is directly proportional to R_t , and the ratio of end-tapped to center-tapped equivalent noise resistances is still about 4.

In all the simulations for Figure 7, the detector current was injected at the input of the preamplifier. An additional effect on signal-to-noise is signal dispersion in the strip. Figure 8 shows the voltage waveforms at the input of the comparator to a 1 fC input charge when the signal is applied at the amplifier-end and at the far-end of the 12 cm strip for an end-tapped, $R_m = 20 \Omega/\text{cm}$, non-irradiated detector. There is a 2.5% reduction in the amplitude of the pulse for the signal injected at the far-end compared with the signal injected at the amplifier-end. This results directly in a 2.5% increase for the worst case ENC. For the center-tap case, the reduction in amplitude due to dispersion is only 0.2%.

Metal Strip Resistance [Ω/cm]	Equivalent Noise Resistance, R_n [Ω]	
	center-tap	end-tap
10	8.4	34.7
15	12.7	51.7
20	16.5	68.7

Table 6: Equivalent noise resistance of the distributed strip resistance for the post-irradiated full detector model.

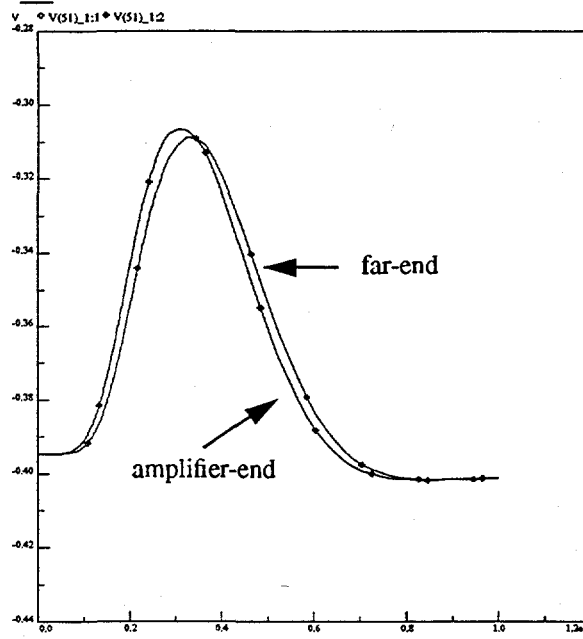


Figure 8. Voltage waveforms at the input of the comparator to a 1 fC input charge when the signal is injected at the amplifier- and far-end of the 12 cm strip for an end-tapped, $R_m = 20 \Omega/\text{cm}$, non-irradiated detector.

Conclusions

From the data in Table 4 and from the signal dispersion information, the worst-case ΔENC (i.e., far-end injection) between end- and center-tapped modules will be 120 to 210 el. rms (9 to 15%) for a non-irradiated detector and 75 to 130 el. rms (5 to 9%) for an irradiated detector, for a metal strip resistance of 10 to 20 Ω/cm .

References

- [1] I. Kipnis, "CAFE: A complementary bipolar analog front-end integrated circuit for the ATLAS SCT," LBNL-39207, May 1995.
- [2] G.C. Temes and J.W. LaPatra, *Introduction to Circuit Synthesis and Design*, McGraw-Hill, 1977, p. 349.